ARTICLE

Theoretical Study of O-Assisted Selective Coupling of Methanol on Au(111)

Bingjun Xu,[†] Jan Haubrich,[†] Thomas A. Baker,[†] Efthimios Kaxiras,[†,‡,§] and Cynthia M. Friend*[,†,‡]

[†]Department of Chemistry and Chemical Biology, Harvard University, Cambridge, Massachusetts 02138, United States
[‡]School of Engineering and Applied Sciences, Harvard University, Cambridge, Massachusetts 02138, United States
[§]Department of Physics, Harvard University, Cambridge, Massachusetts 02139, United States

S *Supporting Information*

ABSTRACT: We report the first systematic theoretical study of the oxidative self-coupling of methanol to form the ester, methylformate, on atomic-oxygen-covered Au(111) using density functional theory calculations. The first step in the process —dissociation of the O—H bond in methanol—has a lower barrier for transfer of the proton to adsorbed oxygen than for transfer of H to gold, consistent with experimental observations that O is necessary to initiate the reaction. The computed barrier for formation of methoxy (CH_3O) and OH is 0.41 eV, compared with 1.58 eV calculated for the transfer of H to the clean Au surface. Several different pathways for the ensuing β-H elimination in CH_3O(ads) to form formaldehyde have been considered, namely, attack by adsorbed O, OH, or a second CH_3O, and transfer to the Au metal. Methoxy attacked by surface oxygen has the lowest calculated barrier, 0.49 eV, and leads to adsorbed $H_2C{=}O$ and OH. Subsequent coupling of methoxy and formaldehyde has no apparent barrier in the calculation, consistent with the experimental conclusion that β-H elimination is the rate-limiting step for the overall reaction. With the exception of surface oxygen, all other surface species have low diffusion barriers, suggesting that rearrangement and movement of these species from the preferred adsorption sites to configurations necessary for reactions occur readily, thus contributing to the activity for coupling on gold.
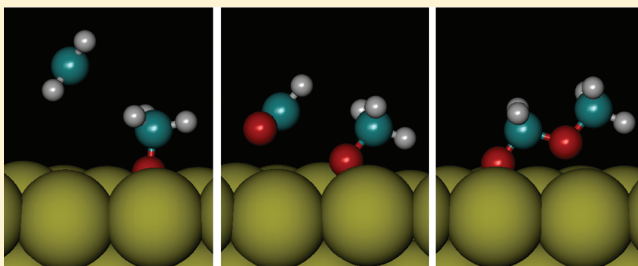
1. INTRODUCTION

Research on Au catalysis has intensified during the past two decades since the discovery that supported Au nanoclusters are extremely active toward low-temperature CO oxidation.[1] Applications of Au-based catalysts have been rapidly expanded to a broad range of reactions, such as alcohol oxidation,[2−14] olefin epoxidation,[15−19] and cross-coupling reactions.[20−23] Alcohol oxidation is of particular interest because it is one of the key transformations in the organic synthesis and in the production of commodity chemicals. Thus, there is the potential for significant energy savings via enhancement of the reaction temperature and selectivity. The current industrialized alcohol oxidation processes are stoichiometric reactions with heavy transition metals, such as Cr^{VI},[24] making Au-based catalysts for such transformations an attractive alternative, employing molecular oxygen as the oxidant with water being a byproduct.[13] Moreover, much lower temperatures are sufficient for oxidation with Au-based catalysts.[2,3,25]

Selective oxidation of alcohols over Au-based catalysts under ambient pressure or liquid phase has been explored extensively with promising results.[10,11,14,25−27] Our previous experimental work under ultrahigh vacuum (UHV) showed that the oxygen-activated Au(111) is able to mediate self-coupling of alcohols[2,3] and cross-coupling between alcohols and aldehydes,[20,21,23] with very high selectivity to the corresponding esters. The catalytic coupling of methanol over metallic, nanoporous gold in the absence of a metal oxide support follows the trends in selectivity predicted from our UHV experiments,[25] establishing the connection between the molecular-level mechanism and a successful catalytic system.

The adsorption and oxidation of alcohol on gold has recently been studied using density functional theory (DFT);[28,29] however, none of the computational studies to date have considered the effect of adsorbed O on activation of the alcohols or the oxidative coupling reactions of alcohols on gold. Theoretical studies can provide deeper insight into the key factors that control reactivity and selectivity.

In previous experimental studies of the self-coupling of alcohols on Au(111), we have established unequivocally that all steps leading to the coupling products *can* be mediated by the Au surface, although the possibility that some steps can also occur in solution cannot be excluded.[30] Atomic oxygen was introduced experimentally to the experimental Au(111) surface by ozone exposure. The O—H bond in the alcohol is activated by reaction with adsorbed atomic oxygen to form an alkoxy, which

Scheme 1. Proposed Reaction Mechanism of Self-Coupling of Methanol on O/Au(111) for Clarity[a]
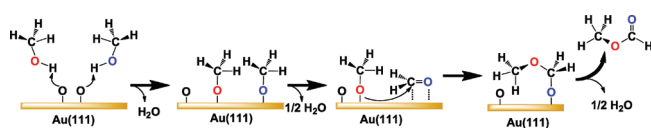
[a] The color coding is used to illustrate the different oxygen species along the reaction pathway, as established by prior experiments. Water, not H_2, is produced in the process.

then undergoes β-H elimination to form the corresponding aldehyde, which, in turn, reacts with another alkoxy to form an adsorbed hemiacetal. From there, β-H elimination from the hemiacetal yields the ester (Scheme 1).[2,3] Given that the elementary steps for the surface-mediated process are well-understood, this is an ideal system for theoretical study, even though it is a complex process.

Herein, we present a DFT study of the elementary reaction steps identified or proposed from these ultrahigh vacuum studies (Scheme 1). Atomic oxygen bound to local 3-fold coordination sites was specifically investigated because it was identified as the preferred binding site at low oxygen coverage, the conditions at which coupling to form the ester is dominant.[2,31,32] Scanning tunneling microscopy studies show that gold is released from the surface to form nanoparticles on the surface. At low oxygen coverage, the surface is decorated by one-atomic high islands about ~2 nm in diameter on top of the Au surface on which the herringbone reconstruction is still evident. Using a combination of DFT calculations and vibrational spectroscopy, we find that the prevalent and most reactive oxygen present under these conditions is bound in the 3-fold fcc sites. Although defects on this surface affect the bond strength of O on the surface, O bound in 3-fold fcc sites is always favored over other adsorption geometries.[32] Because of the complexity of the reaction system under investigation, we focused herein on O in fcc sites on a flat surface and did not explicitly investigate the effect of Au adatoms or other defects on the reactions.[31,32] The possible role of defects would be an interesting topic for future investigation, in particular because under-coordinated Au atoms are thought to facilitate O_2 dissociation[33]—a key step for catalytic processes.

The energetics and reaction barriers that we obtain from the DFT study are consistent with experimental observations and provide a more detailed understanding of the interactions and factors that lead to the selective oxidative coupling on gold. In particular, the key role of atomic O in activating the OH bond in methanol and in the ensuing β-C—H activation of the adsorbed alkoxy is established. The weak interaction of adsorbed intermediates with Au is also a key factor in facilitating coupling.

2. METHODS

All DFT calculations in the present work were performed using the VASP code[34,35] with the GGA-PW91[36] functional to describe electron exchange and correlation. We employed the projector augmented wave (PAW) function method[37] with plane-wave basis sets (cutoff = 400 eV). For reciprocal space, we used a $3 \times 3 \times 1$ Monkhorst—Pack k-point grid. We tested a higher-density Γ-centered $4 \times 4 \times 1$ k-point in several cases and found no significant differences either in adsorption energies or in activation barriers (typical changes in these quantities were

~0.02 eV). The Au(111) surface was modeled by a three-layer slab in the (111) direction, a $p(3 \times 3)$ unit cell in the lateral directions, and a vacuum of 15 Å between slabs; the two upper layers were allowed to relax, with the atoms in the bottom layer fixed at the ideal bulk positions. The bulk gold positions of the bottom layer were taken from the calculated lattice constant of 4.17 Å, which is in good agreement with the experimental value of 4.08 Å.[38] Because insufficient convergence of the slab thickness with respect to properties, such as adsorption and reaction energies, can lead to significant errors, we also tested a $p(3 \times 3)$ four-layer slab model in several cases with the bottom two layers kept frozen, and a $3 \times 3 \times 1$ Monkhorst—Pack k-point grid. The systematic errors in adsorption energies and energy barriers between the three-layer and four-layer slabs are smaller than 0.02 eV. As a result, we conducted the DFT analysis on the three-layer models for computational efficiency. The thickness of the Au slab (3—5 layers) and the number of layers relaxed (1—2 layers) have only a negligible effect on the adsorption energy (Table S2). The dipole correction scheme[39] was tested in the z direction, which is perpendicular to the surface, in many cases, and produced similar deviations ($\Delta E < 0.02$ eV). Thus, no spurious electrostatic interactions between the periodic images are present in the calculations. The electronic structure was converged to within 10^{-4} eV and the geometries optimized until the forces were smaller in magnitude than 0.02 eV/Å. Both spin-polarized and unpolarized calculations were performed when a single H atom is involved in a reaction, and the spin polarization has a negligible impact on the energetics and activation barriers.

We obtain adsorption energies from the total energies of the relaxed surface species relative to the respective isolated and relaxed gas phase molecule/radical and the relaxed clean surface. We do not include any further corrections for coverage and thermodynamic effects due to finite temperature or partial pressure.

We obtained the reaction barriers using the climbing nudged elastic band method (cNEB)[40–42] at a reduced force threshold of 0.05 eV/Å, with at least three images in between the fixed starting and ending points. In several cases, we employed as many as eight images in order to test the convergence of the energy barriers. From the above convergence studies, as well as from previous experience with similar systems, our best estimate for the error bars of activation energies is <0.1 eV. All transition-state structures have been subjected to vibration analysis, and only one imaginary frequency was found along the reaction coordinate.

The activation barriers E_B are defined as the energy difference between the transition state (E_{TS}) and the initial state (E_i), and the thermodynamic barriers E_{Th} are the energy difference between the final state (E_f) and the initial state.

3. RESULTS

3.1. Initial Molecular Activation: Methanol to Methoxy.
The first step in methanol reaction on Au is activation of the O—H bond to form adsorbed methoxy, CH_3O, which has been identified using vibrational spectroscopy.[2] We considered two different reaction routes for dissociative adsorption of methanol to methoxy, with and without the participation of atomic oxygen (eqs 1 and 2, respectively):
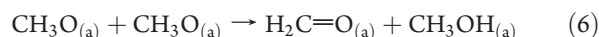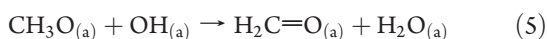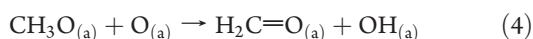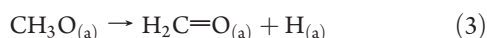
$$CH_3OH_{(a)} + O_{(a)} \rightarrow CH_3O_{(a)} + OH_{(a)} \qquad (1)$$

$$CH_3OH_{(a)} \rightarrow CH_3O_{(a)} + H_{(a)} \qquad (2)$$
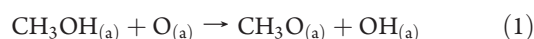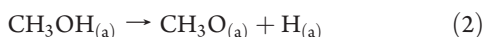
Methanol is more weakly bound to pristine Au(111)-(1 × 1) relative to that containing O: $E_{ads} = 0.15$ eV. When an oxygen adatom is placed in a 3-fold site of the $p(3 \times 3)$ supercell, corresponding to coverage of the surface of $\theta_O = 1/9$ monolayer (ML), methanol preferentially adsorbs on a distorted atop site nearby, gaining ~0.29 eV of additional stabilization via hydrogen bonding (total $E_{ads} = 0.44$ eV).

Experimentally, it *is* observed that atomic O is necessary to activate the O−H bond in methanol and other alcohols, molecular adsorption of methanol being fully reversible on clean Au(111).[2,14] Our calculations also show that O-assisted O−H bond activation has a substantially lower barrier than O−H bond activation by the clean surface alone (Table 1). The high computed reaction barrier, 1.58 eV, for the transition state shown (Figure 1a,b) and the fact that reaction 2 is endothermic by 1.33 eV clearly show that losing a hydrogen atom directly to gold is *not* favorable. The unfavorable thermodynamics are primarily due to the unfavorable bonding of hydrogen atoms to the gold surface.[43,44] Surface oxygen, a strong base, facilitates the formation of methoxy. The presence of the surface oxygen also reduces the thermodynamic reaction barrier (eq 2) from 1.33 to 0.27 eV (eq 1) (see below).

Transfer of H to the neighboring oxygen adatom is facile, as suggested by the computed activation barrier of 0.41 eV. In the transition-state structure, the hydrogen is shared by methoxy and oxygen (Figure 1c,d). The bond lengths in the transition-state structures are summarized in the Supporting Information (Table S1). Methoxy relaxes to an upright configuration, and the hydrogen atom diffuses to a nearby 3-fold site.

The calculated reaction barriers agree qualitatively with experimental observations: no methanol dissociates on clean Au-(111), and instead, it desorbs from the surface molecularly between 130 and 200 K.[14] The results of the DFT studies accurately predict this behavior, as the barrier for desorption is substantially lower than that for dissociative adsorption via O−H bond cleavage (Table 1). That methoxy has been identified on O-covered (111) using vibrational spectroscopy[2] at a surface temperature as low as 160 K is also consistent with the activation energy computed from DFT for the reaction of molecular methanol with adsorbed oxygen of 0.41 eV.

3.2. Methoxy to Formaldehyde. Experimentally, the rate-determining step in formation of methylformate from methanol has been determined to be the transfer of H from the methyl group in methoxy to the surface, the so-called β-H elimination, yielding formaldehyde.[2] There are at least four different possible routes to oxidize methoxy to formaldehyde that cannot be distinguished experimentally (Table 1): (1) transfer of H from methoxy to the Au(111) surface to produce formaldehyde and adsorbed H (eq 3); (2) transfer of H from methoxy to adsorbed oxygen, yielding a transient OH species and formaldehyde (eq 4); (3) transfer of H from methoxy to surface hydroxyl, affording water and formaldehyde (eq 5); and (4) transfer of H from methoxy to a second methoxy, generating formaldehyde and methanol (disproportionation of methoxy) (eq 6).

$$CH_3O_{(a)} \rightarrow H_2C{=}O_{(a)} + H_{(a)} \qquad (3)$$

$$CH_3O_{(a)} + O_{(a)} \rightarrow H_2C{=}O_{(a)} + OH_{(a)} \qquad (4)$$

$$CH_3O_{(a)} + OH_{(a)} \rightarrow H_2C{=}O_{(a)} + H_2O_{(a)} \qquad (5)$$

$$CH_3O_{(a)} + CH_3O_{(a)} \rightarrow H_2C{=}O_{(a)} + CH_3OH_{(a)} \qquad (6)$$

In all pathways considered, methoxy starts from a 3-fold fcc site and then tilts toward the species to which H is transferred, that is, O, OH, methoxy, or the Au surface. In the transition-state structure, H is shared between the carbon atom in the methoxy and the oxygen atom in the species receiving the H such that the difference in the C−H and O−H bond lengths is <0.18 Å.

The formaldehyde produced via these reactions is weakly adsorbed on the surface and does not have a preferred adsorption geometry, which is consistent with previous work.[28] The computed barrier heights for these reaction pathways considered are all similar, ranging between 0.49 and 0.66 eV; however, the thermodynamic energies for the different reactions are substantially different (Table 1). As the range of energies for the calculated barrier heights, 0.17 eV, is nearly in the range of uncertainty in our calculations, no conclusion regarding the preferred pathway can be made based on these differences. However, the range of thermodynamic energies calculated for the products of these reactions is very different, ranging from +0.15 to −1.23 eV.

The most thermodynamically favorable of the reactions is the transfer of a β-H to hydroxyl in an adjacent site (reaction 5) with a computed final energy of −1.23 eV lower than the initial configuration. Transfer of a β-H to either adsorbed O or a second methoxy is also thermodynamically favorable; the product energies relative to the starting reactants are −0.98 and −1.20 eV, respectively (Table 1). Transfer of H directly to gold (reaction 3) is thermodynamically uphill by 0.15 eV (Figure 2; Table 1). The difference in the thermodynamic stability of different pathways is due to the stabilities of the products (e.g., water, OH, or H), instead of the interactions between formaldehyde and other products.

3.3. Esterification. Formation of methylformate, $(CH_3)OC(H){=}O$, from reaction of methoxy and formaldehyde is observed experimentally on O/Au(111).[2,45] The elementary step proposed involves attack of the electron-deficient carbonyl carbon by the electron-rich oxygen in methoxy (eq 7) (Scheme 1).

$$CH_3O_{(a)} + HC({=}O)H_{(a)} \rightarrow CH_3OC({=}O)H_{2(a)} \qquad (7)$$
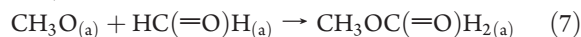
There is no barrier for reaction of methoxy and formaldehyde on Au once the reactants are in the starting configuration shown (Figure 3; Table 1). The final product, adsorbed CH_3OC-$({=}O)H_2$, is more stable by 0.75 eV than the separate reactants (Figure 3 and Table 1). In the starting configuration, the methoxy is bound to a 3-fold site via the O and formaldehyde is weakly bound to the surface ($E_{ads} < 0.1$ eV) and does not have a strong energetic preference for either its orientation or its binding site. The formaldehyde, thus, should approach methoxy in a random direction and orientation. When formaldehyde is close to the methoxy with the carbon end facing the methoxy (Figure 3a,c), the methoxy tilts so the O attacks the electron deficient carbon atom in formaldehyde, resulting in the formation of the alkoxy hemiacetal intermediate, $CH_3OOCH_{2(a)}$, bound to a 3-fold site via the O originally in $H_2C{=}O$ (Figure 3b,d).

The weak binding of formaldehyde to the Au surface facilitates the coupling reaction and probably partly explains the ability of Au to induce coupling. On surfaces with strong binding to the intermediates, the barrier for coupling would be higher because

Table 1. Calculated Activation and Thermodynamic Barriers for Possible Reaction Pathways for Methanol Activation

	reaction pathway	activation barrier[a] (eV)	thermodynamic energy[b] (eV)
	activation of methanol to methoxy		
1	$CH_3OH_{(a)} + O_{(a)} \rightarrow CH_3O_{(a)} + OH_{(a)}$	0.41	0.27
2	$CH_3OH_{(a)} \rightarrow CH_3O_{(a)} + H_{(a)}$	1.58	1.33
	β-H elimination of methoxy to formaldehyde		
3	$CH_3O_{(a)} \rightarrow H_2C{=}O_{(a)} + H_{(a)}$	0.64	0.15
4	$CH_3O_{(a)} + O_{(a)} \rightarrow H_2C{=}O_{(a)} + OH_{(a)}$	0.49	−0.98
5	$CH_3O_{(a)} + OH_{(a)} \rightarrow H_2C{=}O_{(a)} + H_2O_{(a)}$	0.63	−1.23
6	$CH_3O_{(a)} + CH_3O_{(a)} \rightarrow H_2C{=}O_{(a)} + CH_3OH_{(a)}$	0.66	−1.20
	nucleophilic attack of methoxy to formaldehyde to form alkoxy hemiacetal		
7	$CH_3O_{(a)} + HC({=}O)H_{(a)} \rightarrow CH_3OC({=}O)H_{2(a)}$	0	−0.75
	β-H elimination of alkoxy hemiacetal to methylformate		
8	$CH_3OC({=}O)H_{2(a)} + O_{(a)} \rightarrow CH_3OC({=}O)H_{(a)} + OH_{(a)}$	0	−2.18
9	$CH_3OC({=}O)H_{2(a)} + OH_{(a)} \rightarrow CH_3OC({=}O)H_{(a)} + H_2O_{(a)}$	0	−2.33
10	$CH_3OC({=}O)H_{2(a)} \rightarrow CH_3OC({=}O)H_{(a)} + H_{(a)}$	0.22	−0.59

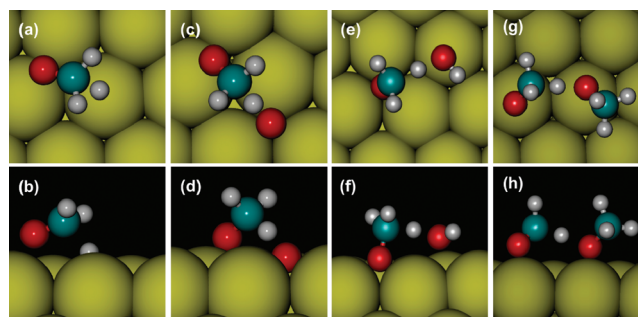[a] The activation barrier (E_B) is defined as the difference between the energy of the transition state (E_{TS}) and the energy of the initial state (E_i); i.e., $E_B = E_{TS} − E_i$. [b] Thermodynamic energy (E_{Th}) is defined as the difference between the energy of the final state (E_f) and the energy of the initial state (E_i); i.e., $E_{Th} = E_f − E_i$.
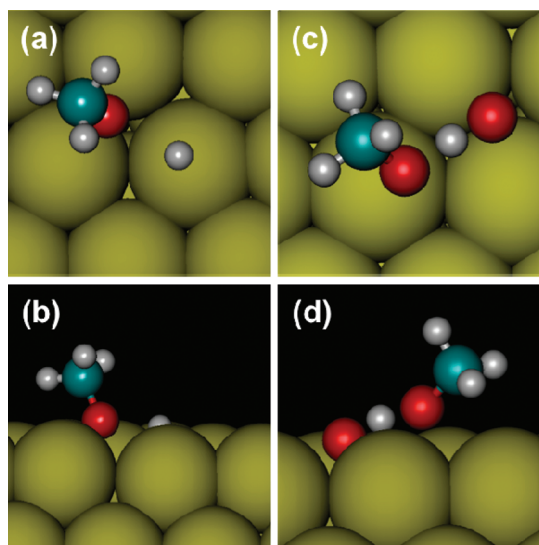
Figure 1. Transition-state structures for transfer of the alcoholic proton of methanol to Au, showing (a) top and (b) side views, and to O adsorbed on Au(111), showing (c) top and (d) side views. The calculations used coverages of 1/9 ML for both O and CH_3OH. Large yellow spheres, red spheres, blue spheres, and small white spheres represent Au, O, C, and H atoms, respectively. The bond lengths are summarized in the Supporting Information (Table S1).

Figure 2. Transition-state structures for formaldehyde formation via β-H transfer from methoxy on Au(111) to Au, showing (a) top and (b) side views; $O_{(a)}$ Au(111), (c) top view and (d) side view; $OH_{(a)}$, (e) top view and (f) side view; and an adjacent methoxy illustrating (g) top and (h) side views. Large yellow spheres, red spheres, blue spheres, and small white spheres represent Au, O, C, and H atoms, respectively. The bond lengths are summarized in the Supporting Information (Table S1).

of the larger energy cost that would be associated with rearranging the reacting species from their most favorable bonding configurations. The other important factor in the coupling is proximity of the reacting species. On Au, this may be achieved through facile diffusion of surface species due to the low diffusion barriers (see below).

Notably, there is no difference in the activation barrier of the formation of the hemiacetal intermediate with or without an oxygen atom at the adjacent 3-fold site (Figure 3; Table 1). The thermodynamic barriers of the formation of the alkoxy hemiacetal intermediate in the absence and presence of an oxygen

atom at the adjacent 3-fold site are also very similar, being −0.70 and −0.75 eV, respectively.

The final step in the formation of methylformate is the loss of a hydrogen atom bound to formaldehyde from the hemiacetal intermediate, based on isotopic labeling experiments.[23] The loss of a hydrogen atom from the hemiacetal to adsorbed O also has no barrier for the starting configuration considered (Figure 4). Furthermore, the reaction pathway described by eq 8 has a large computed energy gain, 2.18 eV.

$$CH_3OC({=}O)H_{2(a)} + O_{(a)} \rightarrow CH_3OC({=}O)H_{(a)} + OH_{(a)} \tag{8}$$
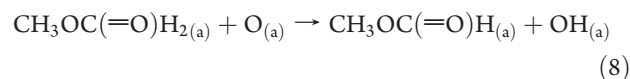
Neither reaction 7 nor reaction 8 has an activation barrier (Table 1), in agreement with the deductions of the experiments that β-H elimination from the methoxy is the rate-limiting step. Replacing $O_{(a)}$ with $OH_{(a)}$ in the β-H elimination of the $CH_3OOCH_{2(a)}$ intermediate, as in eq 9, does
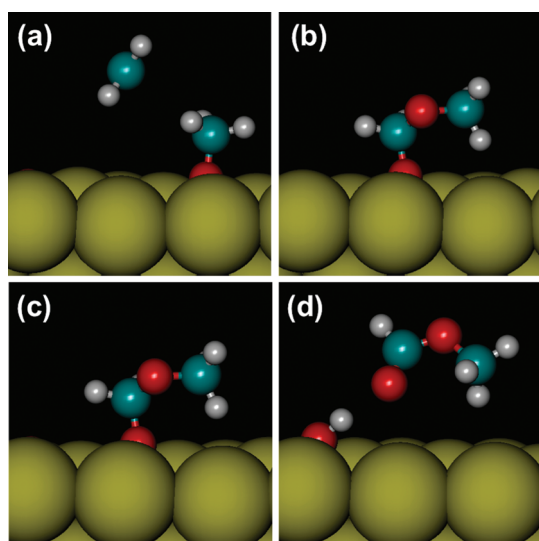
Figure 3. Reaction between methoxy ($\theta_{methoxy}$ = 1/9 ML) and formaldehyde ($\theta_{formaldehyde}$ = 1/9 ML) on the O/Au(111) (θ_O = 1/9 ML) surface leading to the alkoxy hemiacetal intermediate. Panels (a, b) and (c, d) show the side and top views of the starting and end structures of the esterification process, respectively. Representations are the same as in Figure 1.
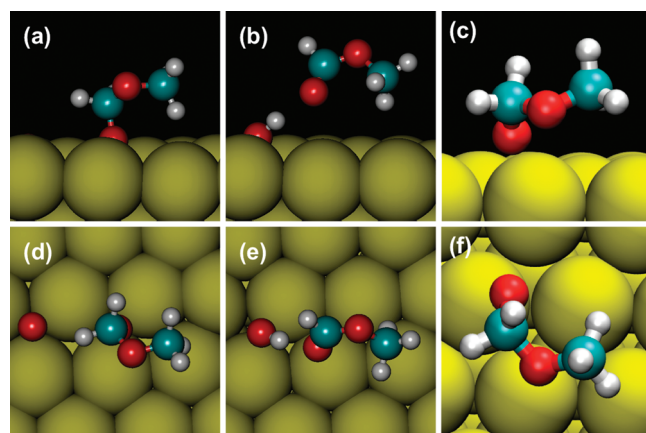
Figure 4. Reaction pathway of the β-H elimination of the alkoxy hemiacetal intermediate ($\theta_{intermediate}$ = 1/9 ML) on the O/Au(111) (θ_O = 1/9 ML) surface. Panels (a, b) and (d, e) show the side view and top view of the starting and end structures of the oxygen-assisted β-H elimination reaction, respectively. Panels (c) and (f) show the side view and top view of the transition-state structure of the surface-assisted β-H elimination reaction. Representations are the same as in Figure 1.

not change the activation barrier.

$$CH_3OC(=O)H_{2(a)} + OH_{(a)} \rightarrow CH_3OC(=O)H_{(a)} + H_2O_{(a)} \tag{9}$$
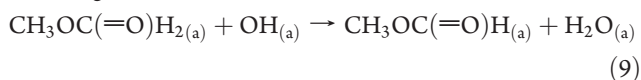
The possible loss of H from the hemiacetal to Au itself, without the involvement of adsorbed O or OH (eq 10), has a modest activation barrier, 0.22 eV (Table 1); this process is exothermic by only 0.59 eV. The transition-state structure is shown in Figure 4c,f. Thus, from both a thermodynamic or kinetic point of view, the reaction described by eq 10 is less favorable than that of eq 8 with surface oxygen. Nevertheless, adsorbed O is *not*

**Table 2. Diffusion Pathways and Barriers on the Surface Species**

surface species	diffusion pathway[a]	diffusion barrier (eV)
methanol and formaldehyde[b]		<0.05
methoxy	3 fold → 2 fold → 3 fold	0.13
alkoxy hemiacetal	3 fold → 2 fold → 3 fold	0.19
O	3 fold → 2 fold → 3 fold	0.46
OH	2 fold → 3 fold → 2 fold	0.10
H	3 fold → 2 fold → 3 fold	0.08

[a] Initial, intermediate, and final bonding sites of the surface species during diffusion. [b] Methanol and formaldehyde only bond to the Au-(111) surface very weakly; no bonding site could be identified.

required for formation of the ester once methoxy and formaldehyde are formed.

$$CH_3OC(=O)H_{2(a)} \rightarrow CH_3OC(=O)H_{(a)} + H_{(a)} \tag{10}$$
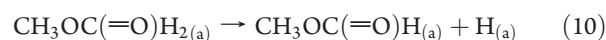
3.4. Hydroxyl and Water. Most of the reaction steps discussed above produce surface hydroxyl as a side product. Previous studies have shown that isolated hydroxyl groups on the Au(111) surface are not stable with respect to disproportionation, but they can coexist in the form of water−hydroxyl surface complexes, as in eq 11.[46]

$$OH_{(a)} + OH_{(a)} \rightleftharpoons H_2O_{(a)} + O_{(a)} \tag{11}$$
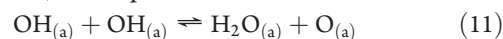
A greatly simplified water−hydroxyl complex model, in which we placed 2/9 ML of OH in the supercell and then calculated the barrier of forming a water molecule and an oxygen adatom, was used to represent the reaction described in eq 11. This model presents a reasonable approximation to the low coverages of water and hydroxyls that we expect from our experiments,[2] although it eliminates most of the hydrogen bonding in the water−hydroxyl−oxygen network. The forward and backward reactions of eq 11 have low activation barriers (0.30 and 0.25 eV), consistent with the high facility and reversibility of both water and hydroxyl formation. Similar results have been reported by Henkelman et al.[47] One key feature of gold catalysis is its low desorption temperature for water. Under previously reported experimental conditions, water leaves the surface immediately,[2] which makes reactions that produce OH or water irreversible.

3.5. Diffusion. All relevant elementary steps in the oxidative coupling of methanol involve two species on the surface at low temperatures (<215 K); therefore, it is important to evaluate the energy cost associated with diffusion on the surface and rearrangement into the starting configurations used for the calculations above. To this end, the cNEB method was used to calculate the diffusion barrier of various surface species (Table 2). The diffusion barriers of most surface species are low enough not to play a significant role in limiting the reaction rate.

The low diffusion barriers of the surface species, which are a consequence of their relatively weak binding to Au, indicate that there is a minimal energetic penalty for assuming the ideal configurations for reaction, thus allowing coupling at relatively low temperatures. Even for reactions involving the relatively strongly bound oxygen, the more weakly bound surface species can efficiently explore the surface; thus, the reaction probability with surface oxygen remains high. Therefore, the reaction rates are more likely limited by the activation barriers of the reactions than by mass transport. kMC calculations using the computed parameters are planned to more quantitatively evaluate this effect.

3707

dx.doi.org/10.1021/jp110835w |*J. Phys. Chem. C* 2011, 115, 3703–3708

4. CONCLUSIONS

We have studied methanol oxidation on oxygen-covered Au(111) using first-principles DFT calculations. The main conclusions drawn from these calculations are the following: (1) surface atomic-oxygen-assisted O−H bond activation is a viable pathway leading to methoxy formation; (2) of the several possible β-H elimination pathways of methoxy to formaldehyde, the lowest activation barrier calculated for activation of the β-C−H bond is that assisted by adsorbed O; (3) activation of the β-C−H bond of methoxy exhibits the highest barrier for any of the steps for the overall reaction, which indicates that it is the rate-limiting step; (4) diffusion for most of the surface species is rapid and facilitates the reactions leading to coupling. Despite this generally good agreement with experiment, a more detailed study including a full treatment of the statistical mechanics through kinetic simulations would be desirable in order to make quantitative comparisons. This issue is beyond the scope of the present work and will be the subject of future investigations.

■ ASSOCIATED CONTENT

Ⓢ Supporting Information.   Bond lengths in the transition-state structure of different reaction steps (Table S1) and the effect of the slab thickness and number of layers relaxed in the slab on the adsorption energy of methanol (Table S2). This material is available free of charge via the Internet at http://pubs.acs.org.

■ AUTHOR INFORMATION

Corresponding Author
*E-mail: cfriend@seas.harvard.edu.

■ ACKNOWLEDGMENT

■ REFERENCES

(1) Haruta, M.; Yamada, N.; Kobayashi, T.; Iijima, S. *J. Catal.* **1989**, *115*, 301–309.

(2) Xu, B.; Liu, X.; Haubrich, J.; Madix, R. J.; Friend, C. M. *Angew. Chem., Int. Ed.* **2009**, *48*, 4206–4209.

(3) Liu, X. Y.; Xu, B. J.; Haubrich, J.; Madix, R. J.; Friend, C. M. *J. Am. Chem. Soc.* **2009**, *131*, 5757–5759.

(4) Della Pina, C.; Falletta, E.; Rossi, M. *Chem. Phys. Chem.* **2009**, *2*, 57–58.

(5) Yang, X.; Wang, X.; Liang, C.; Su, W.; Wang, C.; Feng, Z.; Li, C.; Qiu, J. *Catal. Commun.* **2008**, *9*, 2278–2281.

(6) Wang, X. G.; Kawanami, H.; Dapurkar, S. E.; Veniataramanan, N. S.; Chatterjee, M.; Yokoyama, T.; Ikushima, Y. *Appl. Catal., A* **2008**, *349*, 86–90.

(7) Wang, L. C.; Liu, Y. M.; Chen, M.; Cao, Y.; He, H. Y.; Fan, K. N. *J. Phys. Chem. C* **2008**, *112*, 6981–6987.

(8) Su, F. Z.; Liu, Y. M.; Wang, L. C.; Cao, Y.; He, H. Y.; Fan, K. N. *Angew. Chem., Int. Ed.* **2008**, *47*, 334–337.

(9) Klitgaard, S. K.; DeLa Riva, A. T.; Helveg, S.; Werchmeister, R. M.; Christensen, C. H. *Catal. Lett.* **2008**, *126*, 213–217.

(10) Abad, A.; Corma, A.; Garcia, H. *Pure Appl. Chem.* **2007**, *79*, 1847–1854.

(11) Abad, A.; Almela, C.; Corma, A.; Garcia, H. *Tetrahedron* **2006**, *62*, 6666–6672.

(12) Gong, J. L.; Mullins, C. B. *J. Am. Chem. Soc.* **2008**, *130*, 16458–16459.

(13) Jorgensen, B.; Christiansen, S. E.; Thomsen, M. L. D.; Christensen, C. H. *J. Catal.* **2007**, *251*, 332–337.

(14) Gong, J.; Flaherty, D. W.; Ojifinni, R. A.; White, J. M.; Mullins, C. B. *J. Phys. Chem. C* **2008**, *112*, 5501–5509.

(15) Hutchings, G. J. *Chem. Commun.* **2008**, 1148–1164.

(16) Sinha, A. K.; Seelan, S.; Tsubota, S.; Haruta, M. *Top. Catal.* **2004**, *29*, 95–102.

(17) Lambert, R. M.; Williams, F. J.; Cropley, R. L.; Palermo, A. *J. Mol. Catal. A: Chem.* **2005**, *228*, 27–33.

(18) Deng, X. Y.; Min, B. K.; Liu, X. Y.; Friend, C. M. *J. Phys. Chem. B* **2006**, *110*, 15982–15987.

(19) Hayashi, T.; Tanaka, K.; Haruta, M. *J. Catal.* **1998**, *178*, 566–575.

(20) Xu, B.; Madix, R. J.; Friend, C. M. *J. Am. Chem. Soc.* **2010**, *132*, 16571–16580.

(21) Xu, B.; Haubrich, J.; Fryschlag, C.; Friend, C. M.; Madix, R. J. *J. Chem. Sci.* **2010**, *1*, 310–314.

(22) Xu, B.; Zhou, L.; Madix, R. J.; Friend, C. M. *Angew. Chem., Int. Ed.* **2009**, *49*, 394–398.

(23) Xu, B.; Liu, X.; Haubrich, J.; Friend, C. M. *Nat. Chem.* **2009**, *2*, 61–65.

(24) Sheldon, R. A.; Arends, I.; Ten Brink, G. J.; Dijksman, A. *Acc. Chem. Res.* **2002**, *35*, 774–781.

(25) Wittstock, A.; Zielasek, V.; Biener, J.; Friend, C. M.; Baumer, M. *Science* **2010**, *327*, 319–322.

(26) Miyamura, H.; Matsubara, R.; Miyazaki, Y.; Kobayashi, S. *Angew. Chem., Int. Ed.* **2007**, *46*, 4151–4154.

(27) Dimitratos, N.; Lopez-Sanchez, J. A.; Morgan, D.; Carley, A.; Prati, L.; Hutchings, G. J. *Catal. Today* **2007**, *122*, 317–324.

(28) Chen, W.-K.; Liu, S.-H.; Cao, M.-J.; Yan, Q.-G.; Lu, C.-H. *J. Mol. Struct.: THEOCHEM* **2006**, *770*, 87–91.

(29) Zope, B. N.; Hibbitts, D. D.; Neurock, M.; Davis, R. J. *Science* **2010**, *330*, 74–78.

(30) Abad, A.; Concepcion, P.; Corma, A.; Garcia, H. *Angew. Chem., Int. Ed.* **2005**, *44*, 4066–4069.

(31) Baker, T. A.; Xu, B. J.; Liu, X. Y.; Kaxiras, E.; Friend, C. A. *J. Phys. Chem. C* **2009**, *113*, 16561–16564.

(32) Baker, T. A.; Friend, C. M.; Kaxiras, E. *J. Phys. Chem. C* **2009**, *113*, 3232–3238.

(33) Xu, Y.; Mavrikakis, M. *J. Phys. Chem. B* **2003**, *107*, 9298–9307.

(34) Kresse, G.; Hafner, J. *Phys. Rev. B* **1993**, *47*, 558–561.

(35) Kresse, G.; Hafner, J. *Phys. Rev. B* **1993**, *48*, 13115–13118.

(36) Perdew, J. P.; Wang, Y. *Phys. Rev. B* **1992**, *45*, 13244–13249.

(37) Kresse, G.; Joubert, D. *Phys. Rev. B* **1999**, *59*, 1758–1775.

(38) Lide, D. R., Ed. *CRC Handbook of Chemistry and Physics*; CRC Press: Boca Raton, FL, 1996.

(39) Makov, G.; Payne, M. C. *Phys. Rev. B* **1995**, *51*, 4014–4022.

(40) Sheppard, D.; Terrell, R.; Henkelman, G. *J. Chem. Phys.* **2008**, *128*, 134106.

(41) Henkelman, G.; Uberuaga, B. P.; Jonsson, H. *J. Chem. Phys.* **2000**, *113*, 9901–9904.

(42) Henkelman, G.; Jonsson, H. *J. Chem. Phys.* **2000**, *113*, 9978–9985.

(43) Tierney, H. L.; Baber, A. E.; Kitchin, J. R.; Sykes, E. C. H. *Phys. Rev. Lett.* **2009**, *103*, 246102.

(44) Hammer, B.; Norskov, J. K. *Nature* **1995**, *376*, 238–240.

(45) Outka, D. A.; Madix, R. J. *J. Am. Chem. Soc.* **1987**, *109*, 1708–1714.

(46) Quiller, R. G.; Baker, T. A.; Deng, X.; Colling, M. E.; Min, B. K.; Friend, C. M. *J. Chem. Phys.* **2008**, *129*, 064702.

(47) Ojifinni, R. A.; Froemming, N. S.; Gong, J.; Pan, M.; Kim, T. S.; White, J. M.; Henkelman, G.; Mullins, C. B. *J. Am. Chem. Soc.* **2008**, *130*, 6801–6812.